

Anomalous field-induced growth of fluctuations in dynamics of a biased intruder moving in a quiescent medium

Olivier Bénichou,^{1,*} Carlos Mejía-Monasterio,^{2,3,†} and Gleb Oshanin^{1,‡}

¹*Laboratoire de Physique Théorique de la Matière Condensée (UMR CNRS 7600),
Université Pierre et Marie Curie (Paris 6) - 4 Place Jussieu, 75252 Paris, France*

²*Laboratory of Physical Properties, Technical University of Madrid, Av. Complutense s/n, 28040 Madrid, Spain*

³*Department of Mathematics and Statistics, P.O. Box 68 FIN-00014, Helsinki, Finland*

(Dated: August 13, 2018)

We present exact results on the dynamics of a biased, by an external force \mathbf{F} , intruder (BI) in a two-dimensional lattice gas of unbiased, randomly moving hard-core particles. Going beyond the usual analysis of the force-velocity relation, we study the probability distribution $P(\mathbf{R}_n)$ of the BI displacement \mathbf{R}_n at time n . We show that despite the fact that the BI drives the gas to a non-equilibrium steady-state, $P(\mathbf{R}_n)$ converges to a Gaussian distribution as $n \rightarrow \infty$. We find that the variance σ_x^2 of $P(\mathbf{R}_n)$ along \mathbf{F} exhibits a weakly superdiffusive growth $\sigma_x^2 \sim \nu_1 n \ln(n)$, and a usual diffusive growth, $\sigma_y^2 \sim \nu_2 n$, in the perpendicular direction. We determine ν_1 and ν_2 exactly for arbitrary bias, in the lowest order in the density of vacancies, and show that $\nu_1 \sim |\mathbf{F}|^2$ for small bias, which signifies that superdiffusive behaviour emerges beyond the linear-response approximation. Monte Carlo simulations confirm our analytical results, and reveal a striking field-induced superdiffusive behavior $\sigma_x^2 \sim n^{3/2}$ for infinitely long 2D stripes and 3D capillaries.

PACS numbers: 02.50.-r, 05.40.-a, 66.30.-h, 68.35.Fx

A biased intruder (BI) traveling through a quiescent medium, composed of bath particles which move randomly without any preferential direction, drives the medium to a non-equilibrium steady-state with an inhomogeneous particles' spatial distribution: the latter jam in front of and are depleted behind the BI. The BI can be a charge carrier biased by an electric field or a colloid moved with an optical tweezer. The bath particles may be colloids in a solvent or adatoms on a solid surface.

Such microstructural changes of the medium (MCM) were experimentally observed, e.g., in microrheological studies of the drag force on a colloid driven through a λ -DNA solution [1] or for a BI in a monolayer of vibrated grains [2]. Brownian Dynamics simulations have revealed the MCM for a driven colloid in a λ -DNA solution [1, 3], or for BIs in colloidal crystals [4]. Remarkably, the MCM not only enhance the drag force exerted on the BI, but also induce effective interactions between the BIs, when more than one BI is present [5–8].

The MCM produced by a BI were studied analytically for quiescent baths modeled as hard-core lattice gases with symmetric simple exclusion dynamics [9–15]. Despite some simplifications (interactions are a mere hard-core, no momentum transfer and etc), this type of modeling captures quite well many qualitative features and reproduces a cooperative, essentially many-particle behavior present in realistic physical systems [16, 17]. It is also often amenable to analytical analysis.

It was found that in 1D the size of the inhomogeneity grows in proportion to the traveled distance, so that the jamming-induced contribution to the frictional drag force exhibits an unbounded growth with time n . In consequence, the BI velocity $v_n \propto n^{-1/2}$ [9–11], ensuring

the validity of the Einstein relation for anomalous tracer diffusion in 1D hard-core lattice gases [10–12, 18]. In higher dimensions, the BI velocity approaches a terminal value v and the bath particles' distribution attains a non-equilibrium stationary form with a jammed region in front of the BI and a depleted region in its wake [13–15]. Strikingly, behind the BI the bath particles density approaches the mean value ρ as a power-law of the distance x : $1/x^{3/2}$ and $\ln(x)/x^2$ in 2D and 3D [13–15], which signifies that the medium remembers the passage of the BI on large temporal and spatial scales.

Given such an anisotropy in the bath particles' distribution, one might be curious if the distribution $P(\mathbf{R}_n)$ of the BI vector displacement $\mathbf{R}_n = (X, Y)$ would also be asymmetric along the axis of the applied force. In this paper we address the question of the asymptotic forms of the propagator and provide an exact solution within the lattice gas model with a high bath particles density ρ , (or small density $\rho_0 = 1 - \rho$ of vacancies), i.e. for an *asymmetric* simple exclusion process (ASEP) evolving in a 2D dense sea of symmetric exclusion processes (SEPs).

Using the analytical approach developed previously by two of us in Ref.[19], we set out to show that, curiously enough, in the lowest order in the density of vacancies $P(\mathbf{R}_n)$ along the axis of the applied force tends towards a Gaussian function as $n \rightarrow \infty$. Clearly, when there is no external bias so that the bath is homogeneous, convergence to a Gaussian is quite trivial [20]. In our case, however, given a non-equilibrium situation and essential MCM, this result certainly cannot be expected *a priori*. More striking, we will show that the variance σ_x^2 of $P(\mathbf{R}_n)$ in the direction of the applied bias grows at a faster rate due to an additional logarithmic factor, than

in the direction perpendicular to the force, which is a manifestation of a rather counter-intuitive cooperative behavior. Monte Carlo simulations confirm our analytical results, and reveal a surprising superdiffusive field-induced growth $\sigma_x^2 \sim n^{3/2}$ for infinite 2D stripes and 3D capillaries. On contrary, our simulations show that for single-file geometries σ_x^2 is completely independent of the bias. To the best of our knowledge, these results are new.

Consider a square lattice of $L_x \times L_y$ sites $\mathbf{r} = (x, y)$ with integer valued components and periodic boundary conditions. The lattice is populated with hard-core bath particles and a single hard-core intruder is initially at the origin. M lattice sites are vacant. The system evolves in discrete time n and particles move randomly (subject to hard-core exclusion) by exchanging their positions with the vacancies. The bath particles have symmetric hopping probabilities, i.e., given a vacancy is at an adjacent site, any bath particles exchanges its position with the vacancy with probability $= 1/4$ independently of the direction. On the other hand, the intruder is subject to a constant force \mathbf{F} oriented in the positive x direction. The normalized jump probabilities of the (*isolated*) BI are given, in the usual fashion (see, e.g., Ref.[16]), by

$$p_\nu = \exp\left(\frac{\beta}{2}(\mathbf{F} \cdot \mathbf{e}_\nu)\right) / \sum_\mu \exp\left(\frac{\beta}{2}(\mathbf{F} \cdot \mathbf{e}_\mu)\right), \quad (1)$$

where β is the reciprocal temperature, \mathbf{e}_ν is the unit vector denoting the jump direction, $\nu \in \{\pm x, \pm y\}$, $(\mathbf{F} \cdot \mathbf{e}_\nu)$ is a scalar product and $\mathbf{F} = F \mathbf{e}_x$. The sum with the subscript μ (the normalization constant) denotes summation over all possible orientations of the vector \mathbf{e}_μ .

We turn now to the limit of small density of vacancies, $\rho_0 = M/(L_x \times L_y) \ll 1$, and focus on the behavior in the lowest order in ρ_0 . Then, it is expedient to formulate the dynamics of the system in terms of the dynamics of vacancies. Following Ref.[20], we stipulate that at each tick of the clock each vacancy makes a step exchanging its position with a bath particle chosen at random (with probability $= 1/4$) from among its four neighbors, in case when neither of them is the BI. In case when one of the neighboring particles is the BI, the situation is a bit more complicated. According to Ref. [19] a correct choice of the transition probabilities, which avoids spurious temporal trapping, is as follows: if a vacancy is at site $\mathbf{R}_n + \mathbf{e}_\nu$ at time moment n and the BI occupies site \mathbf{R}_n , then it exchanges its position with the BI with probability $q_{-\nu} = p_\nu/(3/4 + p_\nu)$, and with the probability $= 1/(3 + 4p_\nu)$ with any of three adjacent bath particles. Note that in a complete description of the lattice gas dynamics, these rules would have to be supplemented for cases where two vacancies are adjacent or have common neighbors; however, these cases contribute only to $\mathcal{O}(\rho_0^2)$ so that we can leave the rules for such events unstated.

The steps involved in the derivation of $P(\mathbf{R}_n)$ are discussed in Ref. [19]. In the thermodynamic limit,

($M, L_x, L_y \rightarrow \infty$ with $\rho_0 \ll 1$ kept fixed) the normalized $P(\mathbf{R}_n)$ is given by

$$P(\mathbf{R}_n) \simeq \frac{1}{4\pi^2} \int_{-\pi}^{\pi} d\mathbf{k} \exp(-i(\mathbf{k} \cdot \mathbf{R}_n) - \rho_0 \Omega_n(\mathbf{k})), \quad (2)$$

with $\Omega_n(\mathbf{k})$ defined via its Z-transform :

$$\Omega_z(\mathbf{k}) = \sum_{n=0}^{\infty} \Omega_n(\mathbf{k}) z^n \sim \frac{\Psi(\mathbf{k})}{(1-z)^2 (1 + \chi_z^{-1} \Psi(\mathbf{k}))}, \quad (3)$$

where " \sim " denotes the exact leading at $z \rightarrow 1^-$ ($n \gg 1$) behavior, $\chi_z \sim -\pi/\ln(1-z)$ is the generating function of the mean number χ_n of "new" sites visited at the n -th step (see, e.g., Ref. [20]), $\Psi(\mathbf{k}) = -ia_0 k_x + a_1 k_x^2/2 + a_2 k_y^2/2$ and a_j are given, for arbitrary $\xi = \beta F/2$, by

$$a_0 = \frac{\sinh(\xi)}{(2\pi - 3) \cosh(\xi) + 1}, \quad a_1 = \coth(\xi) a_0, \quad (4)$$

$$a_2 = \frac{1}{\cosh(\xi) + 2\pi - 3}. \quad (5)$$

Differentiating $\Phi(\mathbf{k}) = \exp(-\rho_0 \Omega_n(\mathbf{k}))$ with respect to k_x and k_y , we find that the BI mean velocity v and the variances σ_y^2 and σ_x^2 along the y - and x -axes obey

$$v \sim \rho_0 a_0, \quad (6)$$

$$\sigma_y^2 \sim \rho_0 a_2 n, \quad (7)$$

$$\sigma_x^2 \sim \rho_0 \left(a_1 + \frac{2a_0^2}{\pi} (H_{n+1} - 1) \right) n, \quad (8)$$

where $H_n = \sum_{k=1}^n k^{-1}$ is the n -th harmonic number.

In Fig. 1 (panels *a* and *b*) we present a comparison of our analytical results for the mean velocity and the variance in the y -direction and the results of numerical simulations for fixed bias $\beta F = 5$ and different values of ρ_0 . One notices that our analytical results are in a very good agreement with the numerical data for ρ_0 up to 0.2.

Noticing next that in the large n limit $H_{n+1} \sim \ln(n) + \gamma + \mathcal{O}(1/n)$, where $\gamma \approx 0.577$ is the Euler-Mascheroni constant, we find that asymptotically

$$\sigma_x^2 \sim \rho_0 \left(a_1 + \frac{2a_0^2}{\pi} (\gamma - 1) + \frac{2a_0^2}{\pi} \ln(n) \right) n. \quad (9)$$

On comparing the results in Eqs. (7) and (9), we thus conclude that σ_x^2 grows faster due to an additional logarithmic factor than σ_y^2 , which shows the usual diffusive behavior. It means that, rather counter-intuitively, the distribution becomes progressively more broad along the x direction, compared to its behavior along the y direction. Note that, since $a_0 \sim \beta F$ for $\beta F \ll 1$, the coefficient before the superdiffusive term is proportional to $(\beta F)^2$, which signifies that the superdiffusive behavior emerges beyond (and thus can not be obtained within)

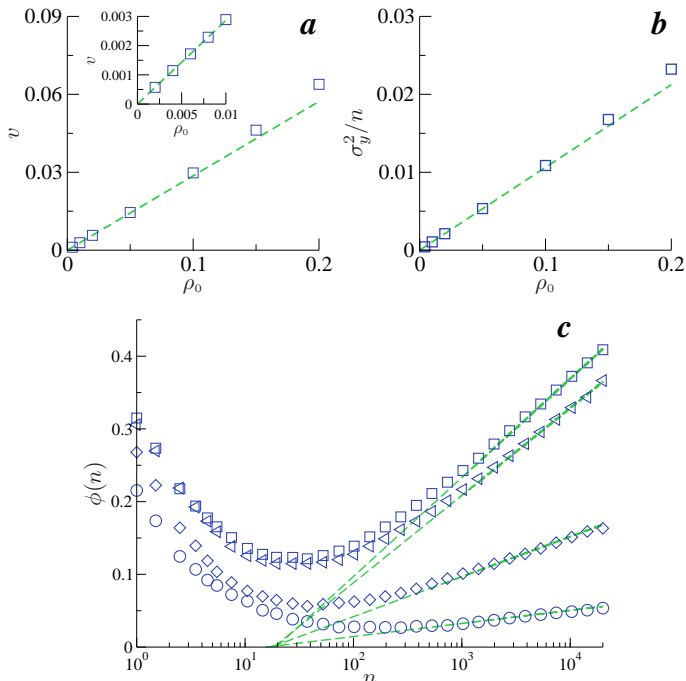


FIG. 1. (color online) Velocity v (panel a) and σ_y^2/n (panel b) versus ρ_0 for $\beta F = 5$. The dashed lines define our theoretical predictions in Eqs. (6) and (7). The symbols are the MC simulations results. The inset in panel a is a zoom of the region $\rho_0 \leq 0.01$. In panel c we plot $\phi(n)$ (see the text) vs n for $\rho_0 = 0.002$, $\beta F = 100$ (\square), $\beta F = 5$ (\triangleleft), $\beta F = 2$ (\diamond) and $\beta F = 1$ (\circ). The dashed curves are our predictions in Eq. (9).

the linear-response approximation.

In Fig. 1 (panel c) we present an evidence for the additional logarithmic factor in the x -component of the variance. To single out this contribution, we plot here versus $\ln(n)$ the function $\phi(n) = \sigma_x^2/n - \rho_0(a_1 + 2a_0^2(\gamma - 1)/\pi)$, which according to Eq. (9) should grow in proportion to $\ln(n)$. One observes an apparent crossover to a logarithmic behavior which persists then over two time decades.

The skewness $\gamma_1(x)$ of $P(X) = \int dY P(\mathbf{R}_n)$ obeys

$$\gamma_1(x) \sim \frac{6a_0(a_0^2 + \pi a_1/\ln(n))}{(2a_0^2 + \pi a_1/\ln(n))^{3/2}} \sqrt{\frac{\ln(n)}{\pi \rho_0 n}}. \quad (10)$$

Note that $\gamma_1(x) > 0$ so that $P(X)$ has a *positive skew* which implies that fluctuations in the BI position are more pronounced for $X > vn$ (i.e. in the region where the bath particles jam) than for $X < vn$ where the bath particles are depleted. Next, for the kurtosis we get

$$\gamma_2(x) \sim \frac{6(4a_0^4 + 6a_0^2\pi a_1/\ln(n) + \pi^2 a_1^2/\ln^2(n))}{(2a_0^2 + \pi a_1/\ln(n))^2} \frac{\ln(n)}{\pi \rho_0 n}, \quad (11)$$

i.e., $\gamma_2(x)$ vanishes as $n \rightarrow \infty$, and hence, $P(X)$ converges to a Gaussian, despite a non-equilibrium and MCM!

We find next that the skewness $\gamma_1(y)$ of $P(Y) = \int dX P(\mathbf{R}_n)$ vanishes. For the kurtosis of $P(Y)$ we obtain $\gamma_2(y) \sim 6 \ln(n)/\pi \rho_0 n$, which implies that $\gamma_2(y)$ decays exactly in the same way as $\gamma_2(x)$ and moreover, $\gamma_2(y)/\gamma_2(x) \rightarrow 1^-$ as $n \rightarrow \infty$. Observe that $\gamma_2(y)$ is *independent* of the bias, while $\gamma_1(x)$ and $\gamma_2(x)$ become *independent* of it when $\ln(n) \gg \pi a_1$.

In Fig. (2) (panels a and b) we compare our analytical predictions for $\gamma_1(x)$ and $\gamma_2(x)$ in Eqs. (10) and (11) against the results of numerical simulations (symbols). To single out the logarithmic factors, we plot here the functions $\tilde{\gamma}_1(x) = n\gamma_1^2(x)$ and $\tilde{\gamma}_2(x) = n\gamma_2(x)$ vs $\ln(n)$. Note that the kurtosis approaches the asymptotic prediction in Eq. (11) quite rapidly, at times of order $n \sim 10^2$ (and moreover, the βF -independent behavior is established quite fast as well). This confirms our result that the kurtosis vanishes as $\gamma_2(x) \propto \ln(n)/n$ and, hence, that the distribution in the direction of the bias converges to a Gaussian. The skewness, which decays at a slower rate, approaches the asymptotic result in Eq. (10) a decade later and the βF -independent behavior sets in at larger times, which are not accessible in our numerical simulations of this essentially many-particle system.

We turn next to the large- (but finite) n corrections to the asymptotic Gaussian distribution. Multiplying both denominator and the nominator of Eq. (3) by the complex conjugate of the denominator, introducing a small parameter $\epsilon_x = a_1 \ln(n)/2\pi\sigma_x^2 \propto 1/n$ ($\epsilon_y = a_2 \ln(n)/2\pi\sigma_y^2 \propto \ln(n)/n$) and expanding $\Phi(k_x, k_y = 0)$ ($\Phi(k_x = 0, k_y)$) up to the second order in ϵ_x (ϵ_y), we get

$$P(X) = \frac{\exp\left(-(\eta_x - \bar{\eta}_x)^2/2\right)}{\sqrt{2\pi\sigma_x^2}} \left\{ 1 + \left[3(g-f) + 6f\bar{\eta}_x^2 - (g+f)\bar{\eta}_x^4 + 2\left(3(g-2f) + (g+2f)\bar{\eta}_x^2\right)\bar{\eta}_x\eta_x - 6(g-f+f\bar{\eta}_x^2)\eta_x^2 - 2(g-2f)\bar{\eta}_x\eta_x^3 + (g-f)\eta_x^4 \right] \epsilon_x + \mathcal{O}(\epsilon_x^2 \ln(n)) \right\}, \quad (12)$$

$$P(Y) = \frac{\exp\left(-\eta_y^2/2\right)}{\sqrt{2\pi\sigma_y^2}} \left\{ 1 + \left[3 - 6\eta_y^2 + \eta_y^4 \right] \frac{\epsilon_y}{2} + \mathcal{O}(\epsilon_y^2) \right\}. \quad (13)$$

where we have conveniently chosen $\eta_x = X/\sigma_x$ ($\eta_y = Y/\sigma_y$), $\bar{\eta}_x = vn/\sigma_x$, $g = 1 + a_0^2 \ln(n)/\pi a_1$ and $f = \pi a_1/2(\pi a_1 + 2a_0^2 \ln(n))$. Note that the result in Eq. (12) becomes identical to that in Eq. (13) when $\beta F = 0$.

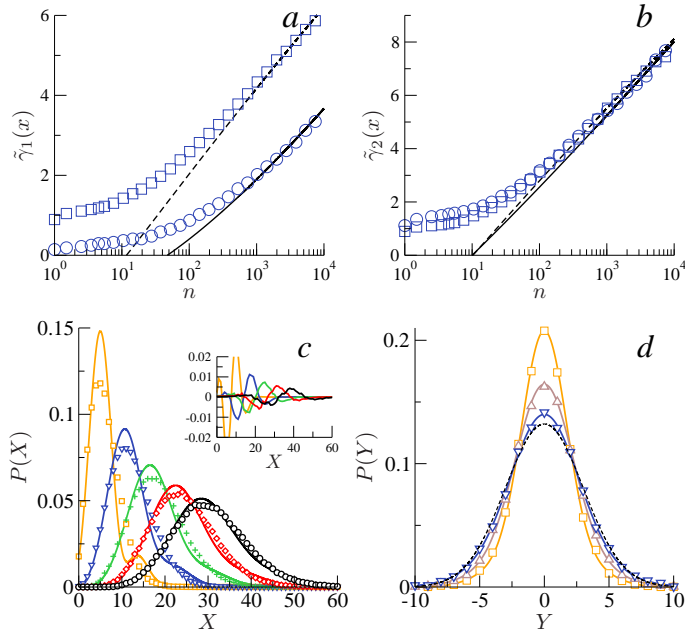


FIG. 2. (color online) Reduced skewness $\tilde{\gamma}_1(x) = n\gamma_1^2(x)$ (panel a) and the kurtosis $\tilde{\gamma}_2(x) = n\gamma_2(x)$ (panel b) for $\rho_0 = 0.002$, $\beta F = 1$ (\circ) and $\beta F = 100$ (\square). Dashed and solid curves are the corresponding theoretical results in Eqs. (10) and (11). Panels c and d present the time evolution of the integrated distributions: $P(X)$ for $\rho_0 = 0.002$ and $\beta F = 100$ for times $n = 10^4$ (\square), 2×10^4 (∇), 3×10^4 ($+$), 4×10^4 (\diamond) and 10^5 (\circ). The inset shows the deviation $\Delta P(X)$ of our result in Eq. (12) from the numerical data. Panel b: $P(Y)$ for $\rho_0 = 0.002$ and $\beta F = 1$ for $n = 10^4$ (\square), 1.5×10^4 (\triangle) and 2×10^4 (∇). Solid curves are our results in Eqs. (12) and (13). The black dashed line defines the asymptotic Gaussian distribution for $n = 2 \times 10^4$.

In Fig. 2 (panels c and d) we compare our Eqs. (12) and (13) against the numerical simulations data. We observe that as time progresses, the discrepancy between Eq. (12) and numerically obtained $P(X)$ gets smaller, as evidenced by the inset in panel c. The convergence is non-uniform so that we have a better agreement between the theory and numerics for the values of X to the left from the maximum, than to the right from it (recall that $\gamma_1(x) > 0$). Along the y -axis (panel d), we observe a pretty good agreement between our Eq. (13) and the numerical data. Note, however, that some slight discrepancy between a Gaussian (blue dashed line) and a Gaussian with the correction term, Eq. (13), persists even for the longest observation time, $n = 2 \times 10^4$.

The following remark is in order: An appearance of the logarithmic factor can be interpreted as a sign that $d = 2$ is the *marginal* dimension for this system, above which (e.g., in 3D) one should expect a usual diffusive

growth of σ_x^2 (with, however, a larger prefactor than in the perpendicular to the bias directions), while in 1D, i.e., for a single-file diffusion, the effect should be stronger and σ_x^2 would get an additional power-law dependence on time. For 3D, indeed, such a scenario seems plausible. We have numerically simulated a BI dynamics in a single-file symmetric lattice gas and realized that, surprisingly, the growth law of σ_x^2 is *not affected* by the bias, i.e., $\sigma_x^2 \sim n^{1/2}$. Moreover, our simulations show that even the prefactor in this dependence is *independent* of βF . On contrary, our preliminary estimates suggest that a strongly superdiffusive behaviour $\sigma_x^2 \sim n^{3/2}$ will take place in quasi-1D systems - infinite two-dimensional stripes ($L_x = \infty$ and finite L_y) and three-dimensional rectangular capillaries ($L_x = \infty$ and finite L_y and L_z). Indeed, our Eq. (9) tells that $\sigma_x^2 \sim n/\chi_n$. By definition, $\chi_n = S_n - S_{n-1}$, where S_n is the mean number of distinct sites visited by any individual vacancy up to time n . For infinite stripes one has $S_n \sim n^{1/2}/L_y$, while $S_n \sim n^{1/2}/L_y L_z$ for infinite rectangular capillaries. Therefore, in both cases we have $\sigma_x^2 \sim n^{3/2}$ which strongly superdiffusive behaviour is unambiguously confirmed by our numerical simulations (see, Fig. 3).

We note finally that a similar superdiffusive behavior $\sigma_x^2 \sim n^\zeta$ with $\zeta \approx 1.45$ has been observed in Molecular Dynamics simulations of a biased intruder dynamics in a glass-forming binary Yukawa liquid in [21] and more recently, in [22]. Taken together, our results and the results of Refs.[21, 22] hint at a possibility of encountering a new physical phenomenon - a field-induced superdiffusive broadening of fluctuations in dynamics of a biased intruder in quiescent molecular crowding environments. This is rather surprising, since such dense environments are commonly associated with a subdiffusive behavior.

We thank K. Binder, S. N. Majumdar, A. Law, F. Ritort, P. Royall, M. Schick, U. Seifert and M. Weiss for helpful discussions. OB acknowledges support from the ERC starting Grant FPTOpt-277998. CMM is

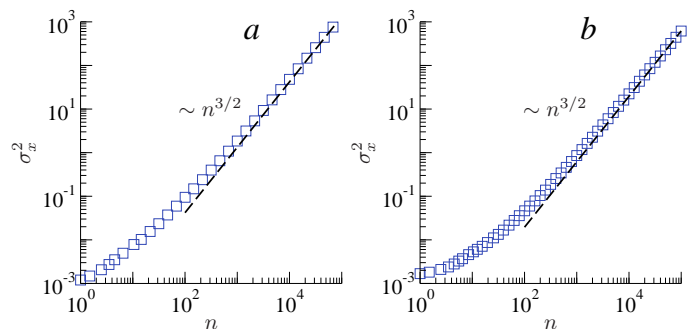


FIG. 3. (color online) Monte Carlo simulations results for the variance σ_x^2 of the BI displacement in stripes with $L_x = 10^4$ and $L_y = 3$ (panel a) and rectangular capillaries with $L_x = 10^4$ and $L_y = L_z = 3$ (panel b) for $\rho_0 = 0.002$ and $\beta F = 100$. The dashed curves in both panels have the slope $n^{3/2}$.

supported by the European Research Council and the Academy of Finland. Partial support from the ESF Research Network "Exploring the Physics of Small Devices" is also acknowledged.

* benichou@lptmc.jussieu.fr

† carlos.mejia@upm.es

‡ oshanin@lptmc.jussieu.fr

- [1] C. Gutsche et al, J. Chem. Phys. **129**, 084902 (2008).
- [2] R. Candelier and O. Dauchot, Phys. Rev. E **81**, 011304 (2010).
- [3] M. Krüger and M. Rauscher, J. Chem. Phys. **131**, 094902 (2009).
- [4] C. Reichhardt and C. J. Olson Reichhardt, Phys. Rev. Lett. **92**, 108301 (2004).
- [5] J. Dzubiella, H. Löwen and C. N. Likos, Phys. Rev. Lett. **91**, 248301 (2003).
- [6] M. Krüger and M. Rauscher, J. Chem. Phys. **127**, 034905 (2007)
- [7] C. Mejía-Monasterio and G. Oshanin, Soft Matter **7**, 993 (2011).
- [8] F. Pacheco-Vázquez and J. C. Ruiz-Suárez, Nat. Commun. **1**, 123 (2010).
- [9] S. F. Burlatsky, G. Oshanin, A. Mogutov and M. Moreau, Phys. Lett. A **166**, 230 (1992).
- [10] S. F. Burlatsky, G. Oshanin, M. Moreau and W. P. Reinhardt, Phys. Rev. E **54**, 3165 (1996)
- [11] C. Landim, S. Olla and S. B. Volchan, Commun. Math. Phys. **192**, 287 (1998)
- [12] G. Oshanin, O. Bénichou, S. F. Burlatsky and M. Moreau, *Instabilities and nonequilibrium structures IX*, (Springer, Dordrecht, Netherlands, 2004), pp. 33–74
- [13] J. De Coninck, G. Oshanin and M. Moreau, Europhys. Lett. **38**, 527 (1997).
- [14] O. Bénichou et al, Phys. Rev. Lett. **84**, 511 (2000); Phys. Rev. B **63**, 235413 (2001).
- [15] O. Bénichou, A. M. Cazabat, M. Moreau and G. Oshanin, Physica A **272**, 56 (1999); O. Bénichou, J. Klafter, M. Moreau and G. Oshanin, Phys. Rev. E **62**, 3327 (2000).
- [16] H. Spohn, *Large Scale Dynamics of Interacting Particles*, (Springer, Berlin, 1991).
- [17] K. Kehr and K. Binder, *Simulations of diffusion in lattice gases and related kinetic phenomena*, in: Applications of the Monte Carlo Methods in Statistical Physics, ed.: K. Binder (Springer, Berlin, 1984), p. 181.
- [18] P. Ferrari, S. Goldstein and J. L. Lebowitz, *Diffusion, Mobility and the Einstein Relation*, in: Statistical Physics and Dynamical Systems, eds.: J. Fritz, A. Jaffe and D. Szasz (Birkhauser, Boston, 1985) p.405
- [19] O. Bénichou and G. Oshanin, Phys. Rev. E **66**, 031101 (2002).
- [20] M. J. A. M. Brummelhuis and H. J. Hilhorst, Physica A **156**, 575 (1989).
- [21] D. Winter, J. Horbach, P. Virnau and K. Binder, Phys. Rev. Lett. **108**, 028303 (2012).
- [22] C. F. E. Schroer and A. Heuer, *Anomalous diffusion of driven particles in supercooled liquids*, ArXiv: 1210.1081